Chapter 12
Print ISBN: 978-93-5547-676-0, eBook ISBN: 978-93-5547-677-7

Analyzing the Effect of Energy Anisotropy on Electromagnetic Ordinary Mode and Purely Transverse Extraordinary Mode

N. Noreen [a*], S. Zaheer [a] and H. A. Shah [a]

DOI: 10.9734/bpi/ntpsr/v3/6103F

ABSTRACT

The effects of energy anisotropy has been analysed for the Ordinary mode (O-mode) and the purely transverse Extraordinary mode (X-mode). By using kinetic theory, the general dispersion relations for O-mode and X-mode have been derived. The stability condition and growth rates have been calculated with the help of energy anisotropy, magnetic field to density ratio (Ω_0/ω_p) and the plasma beta $\beta_\parallel$. The stability of the said modes and the growth rates showt the dependenace of stability on plasma beta $\beta_\parallel$ and energy anisotropy $T_\perp/T_\parallel$. The marginal threshold plasma beta $\beta_\parallel$ and energy anisotropy $T_\perp/T_\parallel$. The marginal threshold O-mode, the dependance of oscillatory and purely growing mode on energy anisotropy are totally opposite to each other.
On the other hand, the X-mode satisfies the instability condition according to difference of geometry with the O-Mode. These modes are important for spherical tokamaks, their coupling leads the generation of the Bernstein mode, which causes the heating effects.

Keywords: Instability; growth rate; anisotropy.

1. INTRODUCTION

The Ordinary mode (O- mode), is a linearly polarized electromagnetic perpendicularly propagating mode. Hamasaki [1,2] investigated the electromagnetic O- mode instability with perpendicularly propagating waves for a two temperature Maxwellian distribution function. Lee [3] studied the same mode in counterstreaming plasmas and showed that the ordinary mode becomes unstable with the change of magnetic field. Later Bornatici and Lee [4] worked on Omode and determined that for counterstreaming plasmas an instability occurs if the streaming velocity exceeds a certain threshold value which can be below the required velocity to excite the electrostatic two-stream instability. They also concluded that an increases in the perpendicular temperature stabilizes the effect and an increase in the parallel temperature enhances the instability. Shivamoggi [5] also discussed the destabilization of the O- mode due to magnetic field and thermal effects. Ibscher et al. [6] investigated the nonresonant Weibel mechanism which can drive the 0 - mode unstable. They studied the instability on the basis of a threshold which gives the instability conditions and upper limits of the growth rate. Their problem was restricted for the fundamental harmonic only. Iqbal et al. [7] studied the O- mode in degenerate anisotropic plasmas and proposed the excitation of a new banded type of instability which grows at some particular values of temperature anisotropy. Hadi et al. [8] also revised the analysis of the O- mode instability with Maxwellian parallel distribution coupled with the thermal ring perpendicular distribution. They demonstrated that O- mode for thermal ring distribution may be excited for cyclotron harmonics as well as for the purely growing branch, depending on the value of the normalized ring speed. Lazar et al. [9] concluded that O- mode instability is driven by an excess of parallel temperature where $A = T_\perp/T_\parallel < 1$ for $\beta_\parallel > 1$ where $\beta_\parallel = \omega_p^2 v_\parallel^2/c^2\Omega_0^2(\omega_p$ is the electron plasma frequency and Ω_0 is the electron cyclotron frequency). Vafin et al. [10] derived the analytical marginal

[a] *Forman Christian College (Chartered University), Ferozpur Road, 54000 Lahore, Pakistan.*
**Corresponding author: E-mail: nailanoreen@fccollege.edu.pk;*

instability condition for magnetized plasmas when charged particles are distributed in counter-streams with equal temperatures. They confirmed the O-mode instability at small plasma beta values, when the parallel counter-stream free energy exceeds the perpendicular bi-Maxwellian free energy. Farrell [11] presented a theory in which he described the direct generation of electromagnetic O- mode emission via mildly energetic electron beams in a highly dense and warm plasma. Khan et al. [12] discussed the propagation characteristics of Omode in relativistic regime with Maxwell- Boltmann-Juttner distribution. They observed that the relativistic plasma environment is more transparent compared to weakly and non relativistic plasma environment. Azra et al. [13] studied the O- mode instability in a Cairns distributed electron plasma. Their results show that the growth rate of O- mode instability is greater for Cairns distribution as compare to the Maxwellian distribution function. They also concluded that in the low density region, a larger value of anisotropy is required to excite the Omode instability .

Lai [14] discussed the Extraordinary mode (X- mode) instability with generalized plasma distribution function. It was shown here that the X-mode instability exists for both low β and high β regimes. The X - mode instability totally depends upon the value of Ω_0^2/ω_p^2. Ali et al. [15] derived the dispersion relation of O- mode and X- mode in ultra-relativistic plasmas by using Maxwellian distribution function. They concluded that the behavior of the said modes is same as in the non-relativistic regime. The damping of the both modes, does not increase for small wave number and is constrained by the present magnetic field. Noureen et al. [16] investigated the dispersion characteristics of X- mode in a relativistic degenerate plasma. They examined the propagation characteristics in different density ranges and found that a shifting of cutoff points due to relativistic effects. The filamentation instability of X-mode is found in laser heating in presence of magnetic field [17], laser produced plasmas where the self generating magnetic field exists [18] and in microwave heating of plasmas [19].

Coupling of the O-mode and X-mode is a necessary tool for generation of the Bernstein mode which is a powerful source of heating in spherical tokamaks. Literature shows the different methods of their coupling, but their unstable regions are major obstacle. Padoba et al. [20] demonstrated the conversion of an O- mode to an X-mode by probe measurements of amplitude and phase of the wave field in the conversion region. Cairns et al. [21] used sheared magnetic field to calculate the linear conversion of the O- mode to the X-mode, since electron Bernstein waves are analyzed as possible candidates for heating spherical tokamaks. Ram et al. [22] developed a kinetic model for studying the energy flow transfer between the X-mode, the O- mode and the electron Bernstein wave in the mode conversion region in the vicinity of the cold plasma upper hybrid resonance. Sodha et al. [23] derived the dispersion relation for modulational instabilities of a Gaussian electromagnetic beam propagating in the two modes O and X-mode, along the externally applied magnetic field, in a homogeneous magnetoplasma.

The work is related to the electromagnetic cyclotron harmonic instability for its possible role in solar and interplanetary radio emission processes where the ratio ω_p/Ω_0 is relatively high i.e., the ratio is of the order of 10 or so and can be as high as 50 or even 100 near 1 a.u. It may be useful for the heating and current drive mechanism in the spherical tori like the NSTX [24] and MAST [25] where the $\omega_p > \Omega_0$. Blagoveshcenskaya et al.[26] discussed the effects of O- mode and X - mode polarized powerful HF radiowaves in high latitude Ionospheric F region. During the experiment, a powerful radiowave of ordinary or extraordinary polarization waves are emitted at fixed frequencies within the range of $4.5 - 8\mathrm{MHz}$ in the direction of the magnetic field.

In this chapter, the energy anisotropic Heaviside distribution function is used for understanding the behavior of O- mode and X- mode. Such type of distribution functions provide detailed information about banded emission of O - mode instability. Such type of emission has been observed in space plasmas, where $\omega_p/\Omega_0 > 10$ (e.g. solar wind). Satellite wave instruments commonly detect banded magnetospheric emissions between harmonics of the electron gyrofrequency in the outer magnetosphere [27]. This type of banded emission has also been observed in the terristial magnetosphere. Frequency-banded electromagnetic waves up to $2000\ \mathrm{Hz}$ are observed concurrently with warm energy-banded ions in the low latitude auroral and sub-auroral zones during every large geomagnetic storm, observed by the FAST and DEMETER satellites. The appearance of the banded

wave activity suggests that there may be distinct changes in the geospace system that characterize large magnetic storms [28].

2. ENERGY ANISOTROPIC HEAVISIDE DISTRIBUTION FUNCTION

The energy anisotropic distribution function, is a cold streaming anisotropic distribution function. The energy anisotropy distribution function is also known as the Waterbag distribution function which consist on the Dirac delta function $\delta(x)$ in the perpendicular direction (ring distribution function) and the Heaviside function $H(x)$ in the parallel direction (unit step distribution function). The Waterbag distribution function was initially introduced by Depackh [29], Morel et al. [30], Feix [31], Bertrand [32], as a bridge between fluid model and kinetic model. Morel et al. [33] used the waterbag distribution function to study the instability threshold of Ion temperature-gradient and they concluded that the results with waterbag distribution are very close to Maxwellian distribution function. The kinetic calculations with waterbag distribution function are more complex compared to the fluid simulations [33]. Schaefer et al. [34] used the same energy isotropic distribution to calculate the relativistic Weibel instability. They concluded that the growth rate of energy anisotropic distribution function is maximum at $k \to \infty$, this is due to the behavior of δ function which is present in the energy anisotropic distribution function. Bertrand et al. [35] discussed non-linear plasma oscillations in terms of waterbag distribution function. According to their results, the use of waterbag distribution is more suitable for computer simulation and provide a simplified description of the Vlasov problem. Yoon and Davidson [36] used the same energy anisotropic distribution function for study of detailed properties of Weibel instability in the relativistic regime. Bashir et al. [37] calculated the Bernstein mode instability and studied its relativistic effects with the energy anisotropic distribution function. According to their results the relativistic effects increases the growth rate of the Bernstein mode. This distribution may find applications in pulsars, relativistic jets like quasars and active galactic nuclei.

The energy anisotropic Heaviside distribution function is given by [36,37]

$$F(p_\perp^2, p_\parallel) = \frac{1}{2\pi\hat{p}_\perp}\delta(p_\perp - \hat{p}_\perp)\frac{1}{2\hat{p}_\parallel}H\left(\hat{p}_\parallel^2 - p_\parallel^2\right) \tag{1}$$

Where $\delta(p_\perp - \hat{p}_\perp)$ is the usual delta function, and $H\left(\hat{p}_\parallel^2 - p_\parallel^2\right)$ Heaviside distribution function which has the following properties

$$\begin{aligned} H(x) &= 1 \text{for} x \geq 0 \\ &= 0 \text{for} x < 0 \end{aligned}$$

And

$$H(x) = \int \delta(x)dx$$

We consider that electrons are evenly spread in the parallel momentum between $-\hat{p}_\parallel \leq p_\parallel \leq +\hat{p}_\parallel = \text{const}$ on the surface. In the relativistic regime the temperature anisotropic Maxwellian distribution function behaves like an energy anisotropic distribution function. For an instability, we require a source of free energy which this distribution function provides free source of energy since this function has streaming in both parallel and perpendicular directions.

This distribution function can also be used to study the Bernstein mode and obliquely propagating X-mode. For parallel propagation this function has been used by Yoon and Davidson [36].

Although we are considering cold plasmas, we may define effective perpendicular and parallel temperatures, in the following standard manner [42]

$$\begin{aligned} T_\perp &= \int d^3p \frac{p_\perp^2}{2m} F(p_\perp^2, p_\parallel) \\ \frac{1}{2}T_\parallel &= \int d^3p \frac{p_\parallel^2}{2m} F(p_\perp^2, p_\parallel) \end{aligned} \tag{2}$$

Using eqn. (1), (2) and performing the perpendicular and parallel integrations, we obtain, we obtain

$$\begin{aligned} T_{\perp} &= \tfrac{1}{2}p_{\parallel}^2 \\ T_{\parallel} &= \tfrac{1}{3}p_{\perp}^2 \end{aligned} \tag{3}$$

3. THE ORDINARY MODE (O- MODE)

The general dispersion relation of the O- mode is as used by [39]

$$N_{\perp}^2 = \epsilon_{zz} \tag{4}$$

where $N_{\perp}^2 = \frac{c^2 k_{\perp}^2}{\omega^2}$

For the sake of completeness, we give below the general description for obtaining the linear dispersion relation of the O- mode by employing the kinetic formulism. Thus we use the Vlasov and Maxwell's equations given by

$$\begin{aligned} &\tfrac{\partial f}{\partial t} + \mathbf{v}\cdot\tfrac{\partial f}{\partial \mathbf{x}} + q\left(\mathbf{E} + \tfrac{\mathbf{v}\times\mathbf{B}}{c}\right)\cdot\tfrac{\partial f}{\partial \mathbf{p}} = 0 \\ &\nabla\times\mathbf{E} = -\tfrac{1}{c}\tfrac{\partial \mathbf{B}}{\partial t} \\ &\nabla\times\mathbf{B} = \tfrac{1}{c}\tfrac{\partial \mathbf{E}}{\partial t} + \tfrac{4\pi}{c}\mathbf{J} \end{aligned} \tag{5}$$

The above may be linearized to obtain the general form of the dielectric tensor given by [40].

$$\epsilon_{ij} = 1 - \tfrac{2\pi}{s} m\omega_p^2 \int_{-\infty}^{\infty} dp_{\parallel} \int_0^{\infty} p_{\perp} dp_{\perp} \chi_1 \sum_{n=-\infty}^{\infty} \tfrac{M_{ij}}{(s + ik_{\parallel}v_{\parallel} + in\Omega)} + L_{ij} \tag{6}$$

where

$$M_{ij} = \begin{bmatrix} \frac{n^2}{z^2} v_{\perp} J_n^2(z) & \frac{in}{z} v_{\perp} J_n(z) J_n'(z) & \frac{n}{z} v_{\parallel} J_n^2(z) \\ -\frac{in}{z} v_{\perp} J_n(z) J_n'(z) & v_{\perp}\left[J_n'(z)\right]^2 & -i v_{\parallel} J_n(z) J_n'(z) \\ \frac{n}{z} v_{\parallel} J_n^2(z) & i v_{\parallel} J_n(z) J_n'(z) & \frac{v_{\parallel}^2}{v_{\perp}} J_n^2(z) \end{bmatrix}$$

and the only non-zero component of L_{ij} is

$$L_{zz} = \tfrac{2\pi}{s^2} m\omega_p^2 \int_{-\infty}^{\infty} dp_{\parallel} \int_0^{\infty} p_{\perp} dp_{\perp} \left[\tfrac{v_{\parallel}}{v_{\perp}}\left(v_{\parallel}\tfrac{\partial f_0}{\partial p_{\perp}} - v_{\perp}\tfrac{\partial f_0}{\partial p_{\parallel}}\right)\right]$$

and

$$\begin{aligned} \chi_1 &= \tfrac{\partial f_0}{\partial p_{\perp}} + \tfrac{ik_{\parallel}}{s}\left(v_{\parallel}\tfrac{\partial f_0}{\partial p_{\perp}} - v_{\perp}\tfrac{\partial f_0}{\partial p_{\parallel}}\right) \\ \hat{z} &= \tfrac{k_{\perp}\hat{p}_{\perp}}{m\Omega_0} = \tfrac{k_{\perp}\hat{v}_{\perp}}{\Omega_0} \end{aligned}$$

Since we are dealing with perpendicular propagation only, we take $k_{\parallel} = 0$, thus the general dispersion relation for perpendicularly propagating O- mode with $k_{\parallel} = 0$ in collionless plasma is given by [41]

$$\begin{aligned} \tfrac{c^2 k_{\perp}^2}{\omega^2} = \; & 1 + \tfrac{2\pi}{\omega}\omega_p^2 \int_{-\infty}^{\infty} p_{\parallel}^2 dp_{\parallel} \int_0^{\infty} dp_{\perp} \chi_1 \sum_{n=-\infty}^{\infty} \tfrac{[J_n(z)]^2}{(\omega - n\Omega_0)} \\ & - \tfrac{2\pi}{\omega^2} m\omega_p^2 \int_{-\infty}^{\infty} dp_{\parallel} \int_0^{\infty} p_{\perp} dp_{\perp} \left[\tfrac{p_{\parallel}}{p_{\perp}}\left(\tfrac{p_{\parallel}}{m}\tfrac{\partial f_0}{\partial p_{\perp}} - \tfrac{p_{\perp}}{m}\tfrac{\partial f_0}{\partial p_{\parallel}}\right)\right] \end{aligned} \tag{7}$$

We now proceed to use the anisotropic distribution function given by eqn. (1), to obtain the ϵ_{zz} component of the dielectric tensor. the consequently upon using eqn. (1) and (7), we get

$$\epsilon_{zz} = 1 - \frac{\omega_p^2}{\omega^2} - \sum_{n=-\infty}^{\infty} \frac{\omega_p^2 \hat{z} J_n(\hat{z}) J_n^{'}(\hat{z})}{\omega(\omega - n\Omega_0)} \frac{2\hat{p}_{\parallel}^2}{3\hat{p}_{\perp}^2} \tag{8}$$

Using eqn. (4), we obtain

$$\frac{c^2 k_{\perp}^2}{\omega^2} = 1 - \frac{\omega_p^2}{\omega^2}\left[1 + \sum_{n=1}^{\infty} \hat{z} J_n(\hat{z}) J_n^{'}(\hat{z}) \left(\frac{2n^2\Omega_0^2}{\omega^2 - n^2\Omega_0^2}\right) \frac{2\hat{p}_{\parallel}^2}{3\hat{p}_{\perp}^2}\right] \tag{9}$$

The above may be simplified to obtain

$$\frac{c^2 k_{\perp}^2}{\omega^2} = 1 - \frac{\omega_p^2}{\omega^2}\left[1 + \sum_{n=1}^{\infty} \frac{\eta_o}{A} \left(\frac{2n^2\Omega_0^2}{\omega^2 - n^2\Omega_0^2}\right)\right] \tag{10}$$

where

$$\eta_o = 2\sum_{n=1}^{\infty} \hat{z} J_n(\hat{z}) J_n^{'}(\hat{z})$$
$$A = \frac{T_{\perp}}{T_{\parallel}} = \frac{\hat{p}_{\perp}^2}{\hat{p}_{\parallel}^2}$$

where the effective temperatures $T_{\perp}$ and $T_{\parallel}$are defined in eqn. (3).

Further for the principle harmonic i.e., $n = 1$, we obtain from eqn. (10)

$$\omega^4 - \left(\Omega_0^2 + c^2 k_{\perp}^2 + \omega_p^2\right)\omega^2 + \omega_p^2 \Omega_0^2 \left(\frac{\hat{z}^2}{A\beta_{\parallel}} + 1 - \frac{\eta_o}{A}\right) = 0 \tag{11}$$

Eqn. (11) is a simpler biquadratic equation and is solved to arrive at the instability condition which is given by

$$\left(\frac{\hat{z}^2}{A\beta_{\parallel}} + 1 - \frac{\eta_o}{A}\right) < 0 \tag{12}$$

This is the general instability condition for both temperature anisotropic Maxwellian distribution and for the energy anisotropic Heaviside distribution function, however our energy anisotropic case A is defined through the effective temperatures (defined in eqn. (3)).

We will consider the stability condition through the anisotropy parameter A, by graphically analyzing eqn. (12) by plotting A versus $\hat{z}$. We see that these plots show banded emission, which is in agreement with the results of Iqbal et al. [7] obtained for an anisotropic Fermi Dirac distribution. The marginal stability condition is obtained by setting the right hand side of eqn. (12) equal to zero and get the dashed red curve. Thus this curve plays the role of threshold value between stable and unstable O- mode.

Below the dotted curve the condition $\frac{\hat{z}^2}{A\beta_{\parallel}} + 1 < \frac{\eta_O}{A}$ is satisfied and the mode is unstable which is presented by dotted blue curve. Above the dashed red curve the condition is $\frac{\hat{z}^2}{A\beta_{\parallel}} + 1 > \frac{\eta_O}{A}$ holds and shows that the 0 - mode is stable above the red curve. The green solid curve shows the stabler O-mode. In all three cases we see the banded nature of the emission.

3.1 Maximum Growth Rate

In this section we compute the maximum growth rate for the O- mode and its dependence on the energy anisotropy.

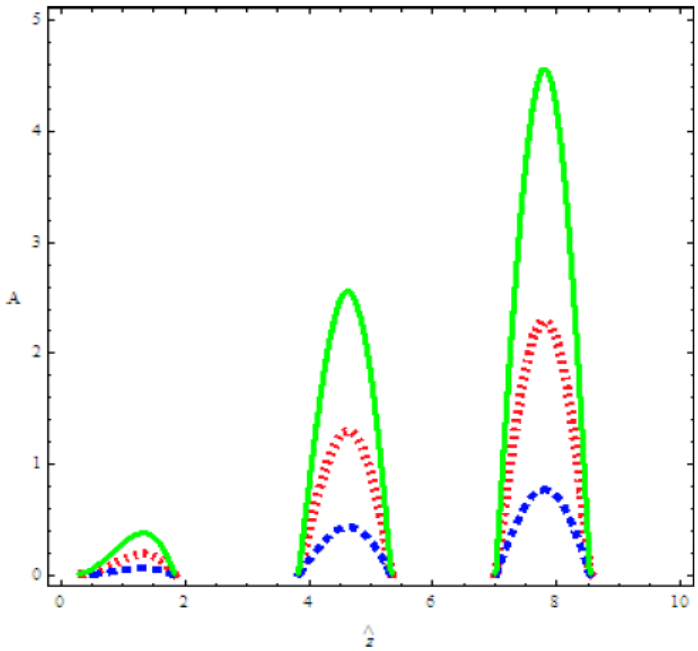

Fig. 1. Marginal Stability Condition

The instability condition was derived in the previous section and is given by eqn. (12). We see that imaginary roots in the small argument limit (of the Bessel function) is given by

$$\omega_i^2 = \frac{\omega_p^2\Omega_0^2\left(\frac{c^2k_\perp^2}{\omega_p^2}+1-\frac{k_\perp^2T_\parallel}{m}\right)}{\Omega_0^2+c^2k_\perp^2+\omega_p^2} \tag{13}$$

The maximum growth rate is obtained in the limit $k_\perp \to \infty$[3], from eqn. (13) and we obtain

$$\omega_{i\max}^2 = \Omega_0^2 - \frac{\omega_p^2T_\parallel}{mc^2}$$

which can also be expressed through the parameter $\beta_\parallel$

$$\frac{\omega_{i\max}^2}{\Omega_0^2} = 1 - \beta_\parallel \tag{14}$$

3.2 Harmonics in the Ordinary mode (O- mode)

Lee [3] discussed O- mode stability for three harmonics with the Maxwellian distribution and the result shows that the said mode is stable for the Maxwellian distribution function. Ichimaru [42] explained the O- mode for higher harmonics with nonlocal effects and confirmed the existence of Azbel- Kaner resonance [43] when the wave frequency is a multiple of electron cyclotron frequency.

The general dispersion relation given by eqn.(10) can be expressed through the parameter $\beta_\parallel$in the following manner

$$\frac{\omega^2}{\omega_p^2} - \frac{\hat{z}^2}{A\beta_\parallel} = 1 + \sum_{n=1}^{\infty}\frac{\eta_o}{A}\left(\frac{2n^2\Omega_0^2}{\omega^2-n^2\Omega_0^2}\right) \tag{15}$$

Now we plot eqn. (15) for different values of the harmonics given by n. We show plots between the normalized real frequency ω/Ω_0 and the parameter $\hat{z}$. Since we consider $\beta_\parallel > 1$ and the $\beta_\parallel$is large

enough to provide a growth rate much larger than the oscillatory frequency $\omega_r << \omega_i$. So these results strongly agree with the solar wind environment [27]. For large anisotropy, $A > 10$, or for $\beta_{\parallel} > 10$, the O- mode instability develops faster than the firehose instability. Larger values of $\beta_{\parallel}$mean smaller magnetic fields or more dense or hotter plasmas, such conditions are frequently attained in different regions of the solar wind.

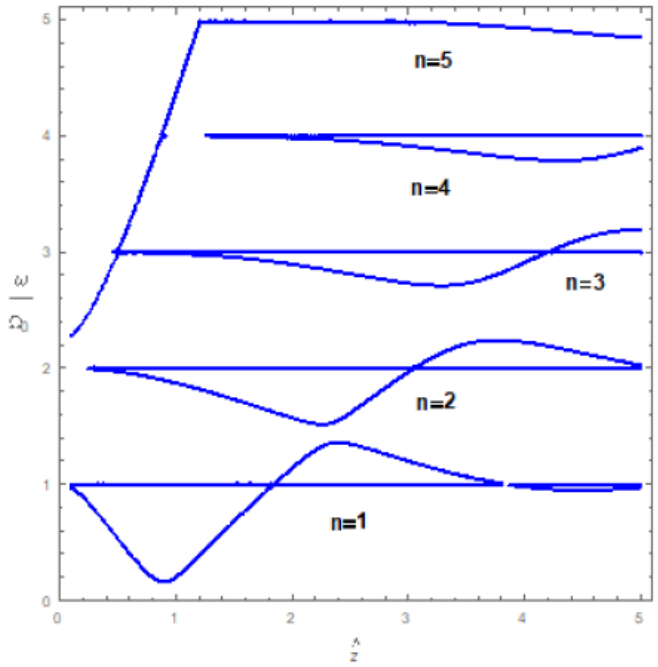

Fig. 2. Stable form of O-mode at $A = 0.1, \beta_{\parallel} = 4.0, \Omega_0^2/\omega_p^2 = 0.25$

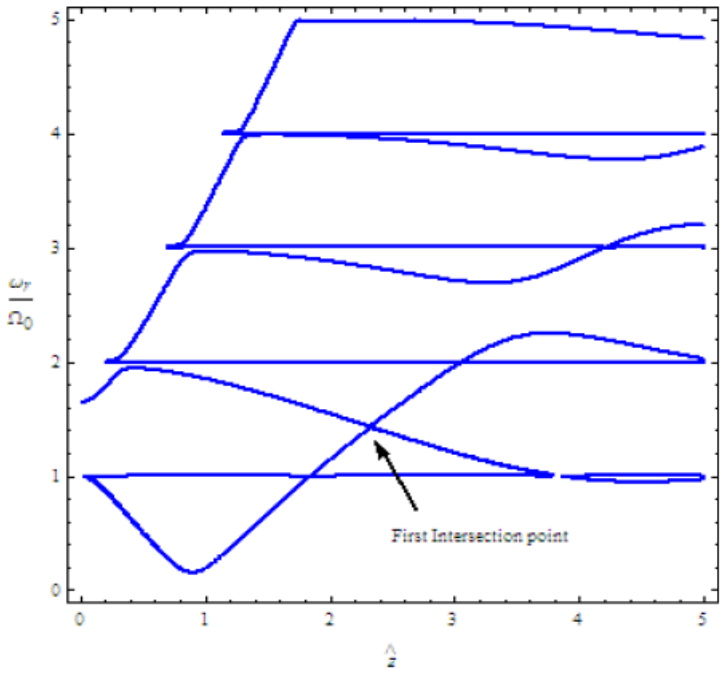

Fig. 3. $A = 0.1, \beta_{\parallel} = 4.0, \Omega_0^2/\omega_p^2 = 0.37$

In Figs. (2-5), the behavior of higher harmonics have been shown for ω_r/Ω_0 vs $\hat{z}$. In Fig. (2), when $A = 0.1$ and $\Omega_0^2/\omega_p^2 = 0.25$, it can be clearly seen that the O- mode is stable and harmonics are not overlapping each other but as we change the value of magnetic field $\Omega_0^2/\omega_p^2 = 0.37$ for same value of anisotropy, harmonics start to intersect each other. In Fig. (3), the intersection point of two harmonics can be clearly observed. On further increasing the value of $\Omega_0^2/\omega_p^2 = 0.43$, it becomes unstable and the first unphysical state is generated as shown in Fig. (4). Fig. (4) and Fig. (5) show the real part of dispersion relation. For analytical threshold, we consider complex form $\omega^2 = (\omega_r + i\omega_i)^2$ in eqn.(15). In the following plots the solid blue lines represent the real frequency ω_r and dashed red lines show the imaginary frequency ω_i, where $\beta_\parallel = 4.0$ for all figures.

These results also satisfy the marginal instability condition as discussed in previous section. In the above plots, the noticeable thing is the value of anisotropy i.e., $A = 0.1$. This shows that the parallel streaming dominates the O- mode and play role in destabilizing the wave and these results also satisfy the high plasma beta regimes.

On further increasing the $\Omega_0^2/\omega_p^2 = 0.60$, unstable regions are obtained and when the value of anisotropy $A = 0.9$, the wave becomes totally unstable as shown in Fig.(5)

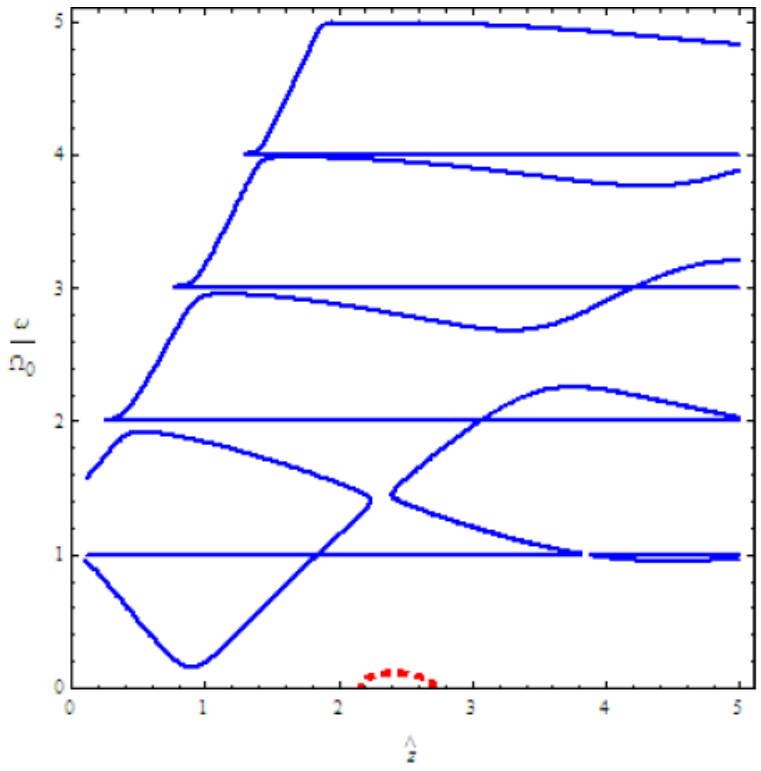

Fig. 4. $\boldsymbol{A = 0.1, \beta_\parallel = 4.0, \Omega_0^2/\omega_p^2 = 0.43}$

The trend of plots show that parallel streaming is responsible in destabilizing the wave and the gaps are produced within the harmonics. The complex part of the dispersion relation shows that the wave is growing in these particular gaps. As in Fig. (5), two gaps are present which means the mode has two unstable regions. In Fig. (6), we have plotted the complex part $\omega_i/\Omega_0 \text{vs} \hat{z}$ which shows the growing part of the second gap of Fig. (5) for different values of anisotropy. We have considered $A = 0.20, 0.33$ and 0.45. For all these three values, the mode is unstable and the growth rate is decreasing with the increasing value of the parallel streaming.

The study of variation of anisotropy tells us that for $T_\parallel > T_\perp$ and $\beta_\parallel > 1$, then wave becomes unstable, this result proves that O - mode instability satisfies the condition of the firehose instability.

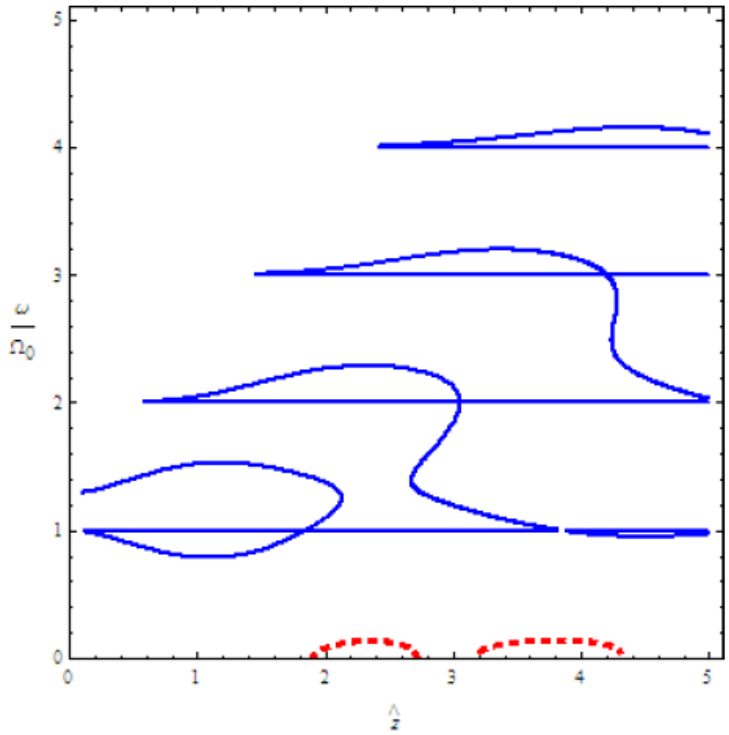

Fig. 5. $A = 0.9, \beta_{\parallel} = 4.0, \Omega_0^2/\omega_p^2 = 0.60$

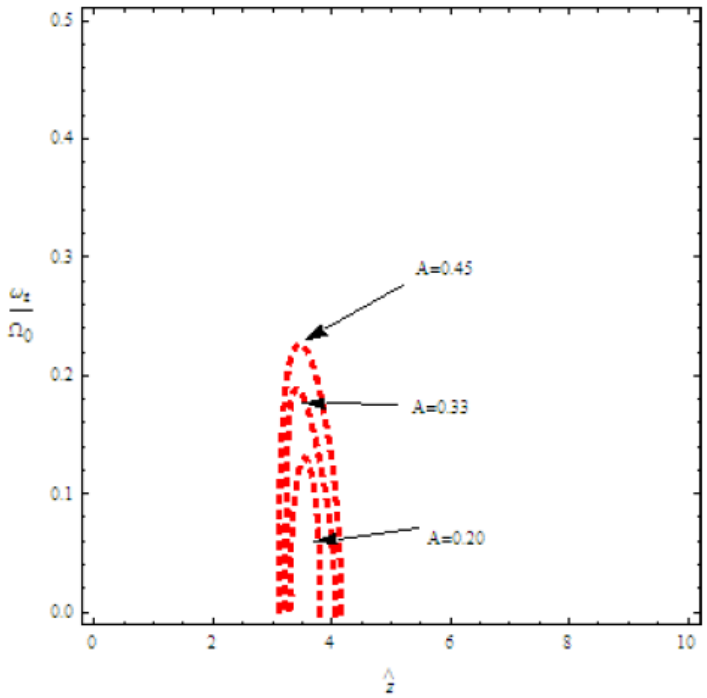

Fig. 6. Growth rate for different values of anisotropy i.e., $A = 0.20, 0.33, 0.45$

3.3 Purely Growing O- mode

The O- mode instability divides in two branches for complex ω. First branch is called oscillatory mode when $\omega_i = 0$ and second branch is aperiodic or purely growing mode when $\omega_r = 0$ as in Fig. (7).

Further increasing the value of parallel streaming, the aperiodic branch is obtained. For oscillatory branch the magnetic field plays a role to destabilize the wave and increase the growth rate of the wave. Similarly, for purely growing mode, the increasing value of magnetic field follows the same trend. But the anisotropy has very small value i.e., $A = 0.09$, means the parallel streaming is much larger than the perpendicular streaming.

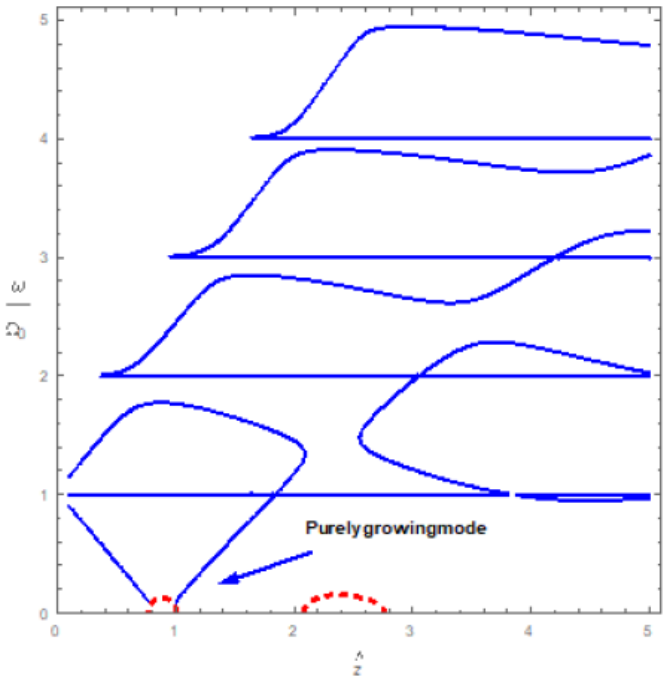

Fig. 7. $\boldsymbol{A = 0.09, \quad \Omega_0^2/\omega_p^2 = 0.9, \beta_{\parallel} = 4.0}$

For aperiodic or purely growing mode, the trend is opposite to the oscillatory mode. For higher values of parallel streaming, the growth rate is also high. So the results of the purely growing mode contradicts with oscillatory mode that the growth rate of purely growing O- mode is increasing for increasing value of parallel streaming. Fig. (8) shows the increasing growth rate of aperiodic mode with increasing value of parallel streaming. We note that this part also satisfies the condition of the firehose instability i.e., $T_{\parallel} > T_{\perp}$ and $\beta_{\parallel} > 1$. The purely growing wave is also called non-propagating firehose instability [44].

4. THE EXTRAORDINARY MODE (X-Mode)

The general dispersion relation of the pure transverse X - mode is [38]

$$N_{\perp}^2 = \epsilon_{yy} \qquad (16)$$

.By using the same generalized dielectric tensor and using the energy anisotropic distribution function, the dispersion relation of the X - mode can be written as

$$\frac{c^2 k_{\perp}^2}{\omega^2} = 1 - \frac{\omega_p^2}{\omega^2} \sum_{n=1}^{\infty} \eta_x \left(\frac{2\omega^2}{\omega^2 - n^2 \Omega_0^2} \right) \qquad (17)$$

which in terms of anisotropy parameter A and $\beta_{\parallel}$can be expressed as

$$\frac{\omega^2}{\omega_p^2} - \frac{\hat{z}^2}{A\beta_{\parallel}} = \sum_{n=1}^{\infty} \eta_x \left(\frac{2\omega^2}{\omega^2 - n^2 \Omega_0^2} \right) \qquad (18)$$

where

$$\eta_x = \left[2\hat{z}J_n^{'}(z)J_n^{''}(z) + 2\left[J_n^{'}(z)\right]^2\right]$$

For higher harmonics, the X-mode is also unstable but in the case when the perpendicular streaming dominates i.e., $T_\perp > T_\parallel$. The wave becomes unstable for large values of perpendicular streaming. In Fig. (9), from eqn. (18), when $A = 6.5$, the wave is stable. But when $A = 6.96$, the harmonics start to overlap each other and wave becomes unstable as shown in Fig. (10). We have considered the same value plasma beta $\beta_\parallel = 4.0$ that we have used in O-mode case, these parameters holds for the solar wind [27] means this is the same regime of the solar wind. We have followed the formulation as way done for the O- mode.

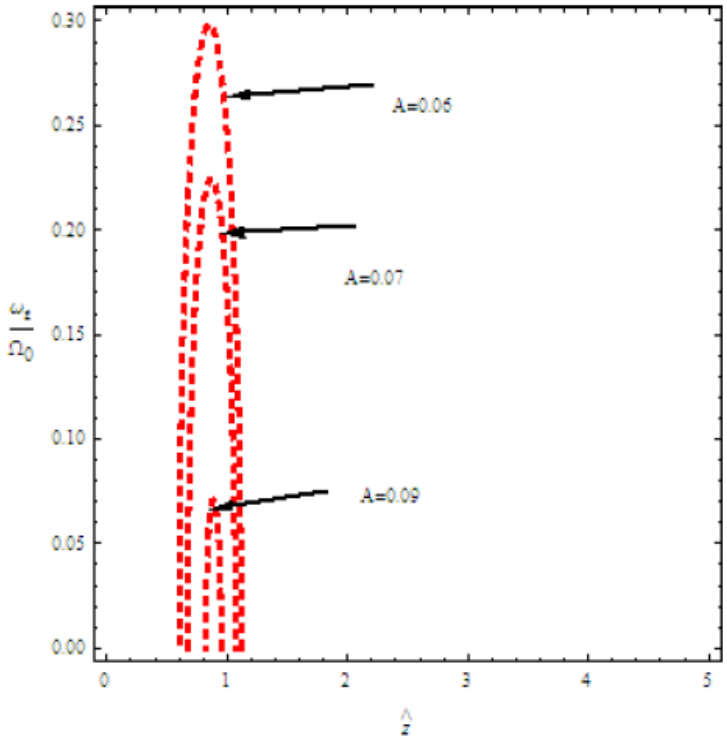

Fig. 8. Growth rate for aperiodic branch for different valus of anisotropy i.e., $A = 0.09, 0.07, 0.06$

On further increasing the value of perpendicular streaming, the mode becomes more unstable as shown in Fig.(11) where the value of $A = 8$ and $\Omega_0^2/\omega_p^2 = 0.09$. The solid blue lines show the real part of the wave and dashed red lines show the growing part of the X - mode. Thus for large values of A, the X - mode is unstable and perpendicular streaming dominates. At $A = 11$, the X - mode becomes totally unstable Fig. (12).

Further, we find the growth rate of the X- mode by plotting ω_i vs $\hat{z}$ from eqn. (18). The imaginary part of ω reveals the detail about the gaps present within the harmonics. In these particular gaps, the wave becomes unstable and the imaginary part gives the growth rate of the unstable regions shown by red dotted lines Figs. (11) and (12).

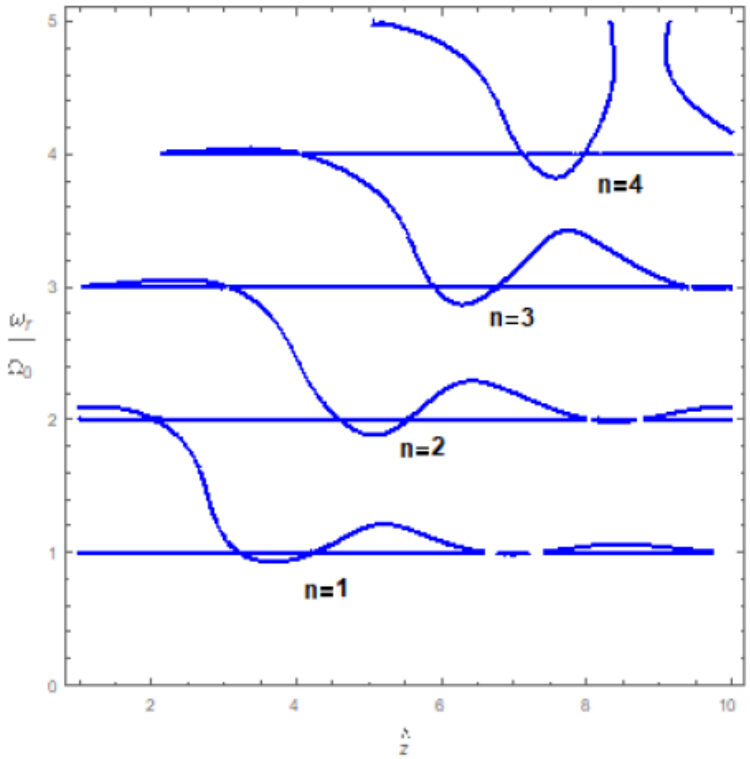

Fig. 9. Stable form of the X-mode at $A = 6.5$, $\Omega_0^2/\omega_p^2 = 0.09$, $\beta = 4.0$

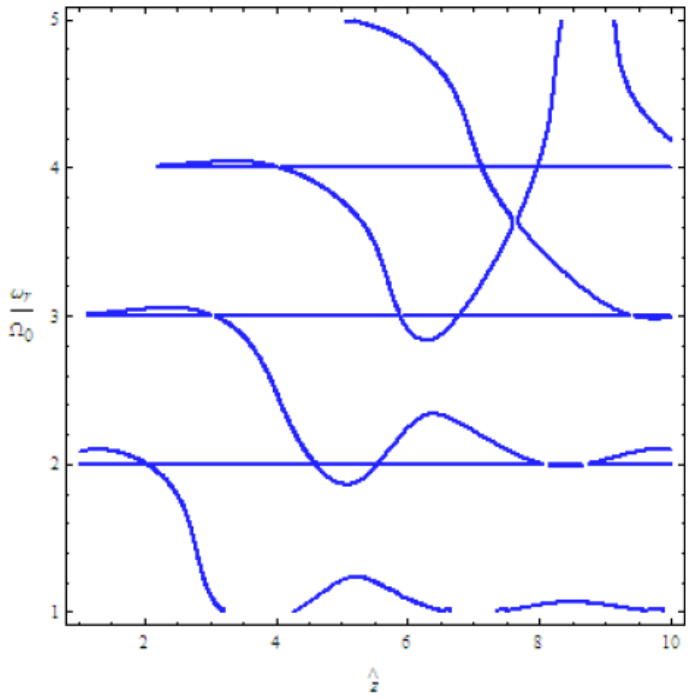

Fig. 10. A= 6.69, $\Omega_0^2/\omega_p^2 = 0.09 \qquad \beta = 4.0$

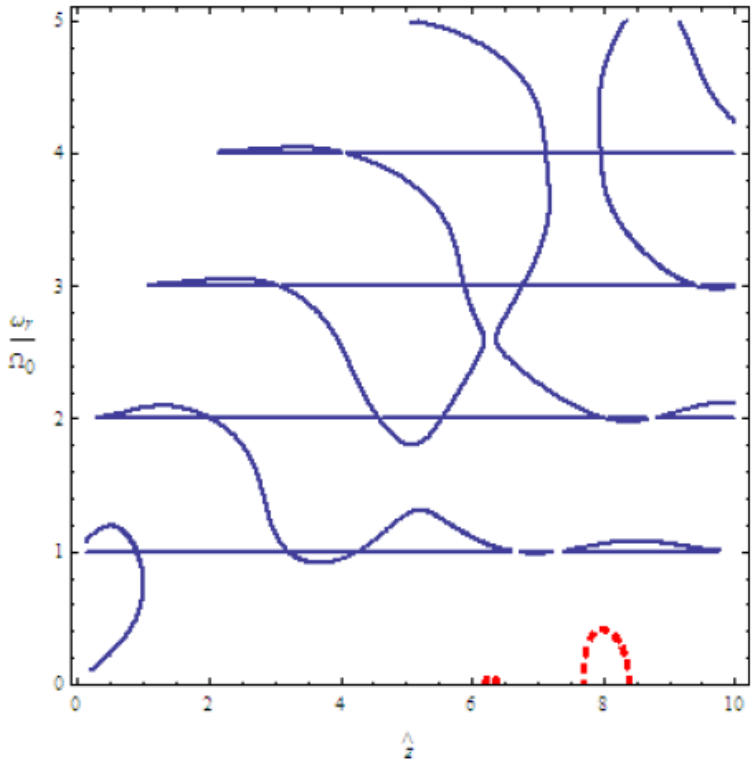

Fig. 11. $A = 8.0, \quad \Omega_0^2/\omega_p^2 = 0.09, \quad \beta = 4.0$

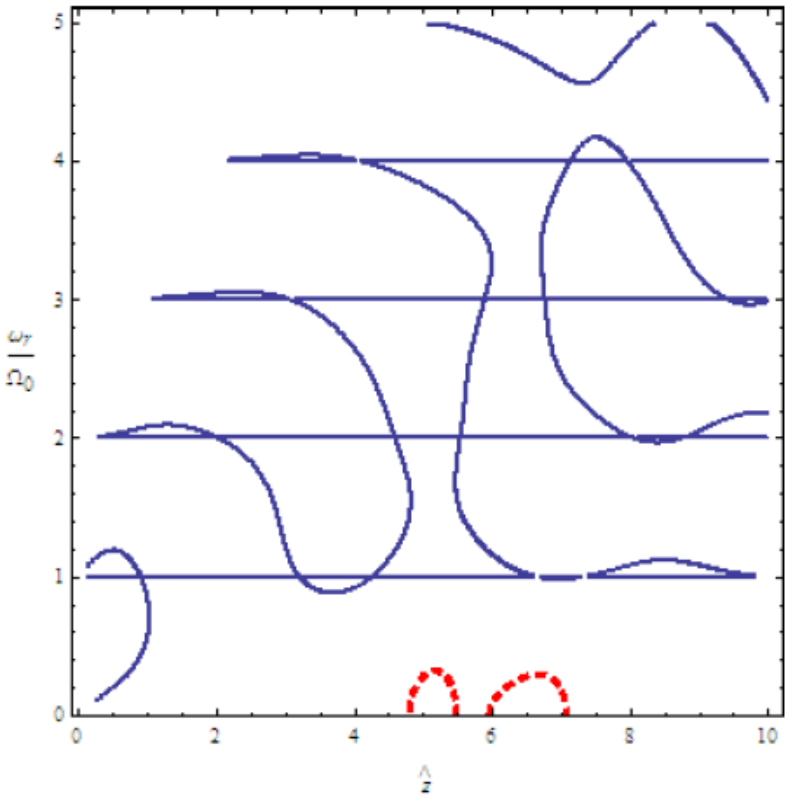

Fig. 12. $A = 11, \quad \Omega_0^2/\omega_p^2 = 0.09, \quad \beta = 4.0$

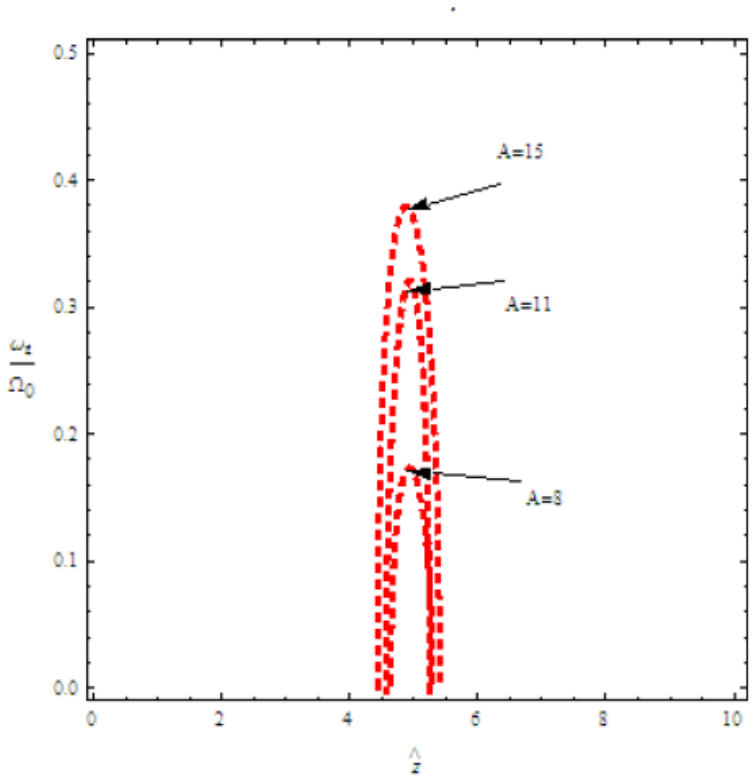

Fig. 13. Growth rate of X-mode for different values of anisotropy i.e., $A = 8, 11, 15$

Fig. (13), shows the imaginary part of ω in the first gap of Fig. (12) for different values of anisotropy. We see that the perpendicular streaming dominates i. e., $T_\perp > T_\parallel$ and by increasing value of perpendicular streaming, the growth rate also increases.

4. CONCLUSION

O- mode instability, for principle harmonic depends upon the magnetic field even where it is weak $\Omega_0^2/\omega_p^2 < 1$. The growth rate varies directly with the value of anisotropy $A = T_\perp/T_\parallel$. We have calculated the marginal threshold condition in form of plasma parameters A and $\beta_\parallel$for principle harmonic. For higher harmonics, oscillatory mode become unstable for $T_\parallel > T_\perp$, as well as the purely growing part. Graphical analysis shows that the parallel streaming dominates in both oscillatory and purely growing mode. With the decreasing value of parallel streaming, the growth rate of oscillatory mode is increases but decreases in purely growing mode. The oscillatory and purely growing mode both satisfies the conditions of firehose instability i.e., $T_\parallel > T_\perp$ and $\beta_\parallel > 1$ as $B_0 \parallel E$ in O- mode. The stability analysis of the X- mode shows that the perpendicular streaming dominates. The mode is unstable for $T_\perp > T_\parallel$, according to geometry of the X - mode that is $B_0 \perp E$. The growth rate of the X - mode increases with the increasing value of perpendicular streaming $T_\perp$.

COMPETING INTERESTS

Authors have declared that no competing interests exist.

REFERENCES

1. Hamasaki S. Electromagnetic microinstabilities of plasmas in a uniform magnetic induction. Phys. Fluids. 1968;11:12.

2. Hamasaki S. Stability of electromagnetic waves propagating perpendicular to a uniform magnetic induction. Phys. Fluids. 1968;6:11.
3. Lee KF. Phys. Rev. 1969;1:181.
4. Bornatici M, Lee KF. Stability analysis of electromagnetic ordinary and extraordinary modes. Phys. Fluids. 1971;13:42.
5. Shivamoggi BK. Instability of the electromagnetic ordinary mode in counterstreaming plasmas. Astrophys. and Space sci. 1982;82:481.
6. Ibschar D, Lazar M, Schlickeiser R. Phys. Plasmas. 2012;190:72116.
7. Iqbal Z, Hussain A, G. Murtaza NL. On the ordinary mode and whistler mode instabilities in the degenerate anisotropic plasmas. Tsintsadze. Phys. Plasmas. 2014;21:032128.
8. Hadi F, Yoon PH, Qamar A. Phys. Plasmas. 2015;22:022112
9. Lazar M, Schlickeiser R, Poedts S, Stockem A, Van S. arXiv: Phys. Plasmas. 2014; 2:1411.1508.
10. Vafin S, Schlickeiser R, Yoon PH. Marginal instability threshold condition of the aperiodic ordinary mode in equal-mass plasmas. Phys. Plasmas. 2014;21:104504.
11. Farrell WM. J. Geophys. Res. 2001;106:15701.
12. Khan W, Ali M, Habib Y. Characteristics of ordinary mode in fully relativistic electron plasma. Plasma Phys. Control. Fusion. 2020;62:055016.
13. Azra K, Z. Iqbal, G. Murtaza Commun., Theor. Phys. 2018;69:699.
14. Lai CS. Phys. of Plasma. 1976;19:575
15. Ali M, Zaheer S, Murtaza G. Prog. theor. Phys. 2010;124:6.
16. Noureen S, Abbas G, Sarfaraz M. Phy. Plasmas. 2018;25:012123.
17. Steinhaur LC. Phys. Fluids. 1976;191740.
18. Stamtjer JA, Bondner SE. Phys. Rev.Lett. 1976;37:435.
19. Porkolab M. Physica. 1976;82C:86.
20. Podoba YY, Laqua HP, Warr GB, Schubert M, Otte M, Marsen S, Wagner F. Phys. Rev. Letter. 2007; 98:255003.
21. Cairns RA, Lashmore- Daviesa CN. Phys. Plasmas. 2000;7:10.
22. Ram AK, Bers A, Lashmore- Davies CN. Emission of electron Bernstein waves in plasmas. Phys. Plasmas. 2002;9:409.
23. Sodha MS, Sharma RP, Maheshwari KP, Kaushik SC. Phys. Plasmas. 1977;20585
24. Ono M, et al. Nucl. Fusion. 2004;44:452
25. Akers RJ, et al. Phys. Plasmas. 2002; 9:3919.
26. Blagoveshchenskaya NF, et al. Cosmic Res. 2018; 56:11.
27. Colpitts CA, Cattell CA, Kozyra JU, Parrot M. J. Geophys. Res. 2012;117:10.
28. LaBelle J, D. R. Ruppert, R. A. Treumann, J. Geophys. Res. 1999;104:293.
29. DePackh DC. J Electron Contro. 1962;13:417.
30. Morel P, et al. Phys. of Plasmas. 2011;18:032512.
31. Feix MR, F. Hohl, L. D. Staton,Nonlinear effects Plasmas. 1969;03
32. Bertrand P, Feix MR. Phys Lett. 1968;28A:68.
33. Bertrand P, Feix MR. Frequency shift of non linear electron plasma oscillation. Phys Lett. 1969;29A:489.
34. Morel P, Gravier E, Besse N, Ghizzo A. p. Bertrand, Comm. non-lin. Sci. Num. Simul. 2008; 13:11.
35. Schaefer-Rolffs U, Tautz RC. Phys. of Plasmas. 2008;15:062105.
36. Bertrand P, M. Gros, G. Baumann, (1976), Phys. of Fluid. 1976;19:1183.
37. Yoon PH, Davidson RC. Phys. Rev. A. 1987;35:2718
38. Bashir MF, N. Noreen, G. Murtaza, Yoon PH. Phys. Plasma and contll. Fusion. 2014;565.
39. Davidson RC. Kinetic waves and Instabilities in aUniform Palsma, North Holland Company. 1983;01.
40. Krall NA, A. Trivelpiece W. Principles of Plasma Physics, McGraw-Hill LTD, Tokyo; 1932.
41. Bashir MF, Murtaza G. Braz., J. Phys. 2012;42:487.
42. Ichimaru S. Basic Principles of Plasma Physics A statistical approach, Addison-Wasley Publishing Company, New York, 104M; 1973.
43. Langenberg DN, Marcus SM. Topology of fermi surfaces of metals (reference table). Phys. Rev. Journ. 1964;136:1383.
44. Lazar M, Poedts S, Schlickeiser R, Ibscher D. arXiv, Solar Phys; 2013.

Biography of author(s)

N. Noreen
Forman Christian College (Chartered University), Ferozpur Road, 54000 Lahore, Pakistan.

Research and Academic Experience: She has 13 years of Experience.

Research Area: Theoretical Plasma Physics.

Number of Published papers: She has 10 Published papers.

Special Award: She is a Silver Medallist in Masters. Distinction in PhD

S. Zaheer
Forman Christian College (Chartered University), Ferozpur Road, 54000 Lahore, Pakistan.

Research and Academic Experience: She has 20 years of Experience.

Research Area: Theoretical Plasma Physics.

Number of Published papers: She has 22 Published papers.

H. A. Shah
Forman Christian College (Chartered University), Ferozpur Road, 54000 Lahore, Pakistan.

Research and Academic Experience: He is a Prof of Physics. He has been Teaching since 1986 and served as Vice Chancllor Government College University Lahore.

Research Area: Theoretical Plasma Physics.

Number of Published papers: He has 145 research articles in the national and international journals.

Special Award: He received Civil Award (sitara e imtiaz) by the Government of Pakistan; Fellow Pakistan Academy of Sciences.

DISCLAIMER
This chapter is an extended version of the article published by the same author(s) in the following journal.
Journal of Modern Physics, 7, 1120-1131, 2016.